



HAL
open science

Vulnerability of a reinforced concrete wall loaded by a snow avalanche: experimental testing and FEM analysis

I. Ousset, D. Bertrand, M. Brun, A. Limam, M. Naaïm

► To cite this version:

I. Ousset, D. Bertrand, M. Brun, A. Limam, M. Naaïm. Vulnerability of a reinforced concrete wall loaded by a snow avalanche: experimental testing and FEM analysis. International Snow Science Workshop (ISSW), Oct 2013, Grenoble – Chamonix Mont-Blanc, France. p. 892 - p. 899. hal-00951668

HAL Id: hal-00951668

<https://hal.science/hal-00951668v1>

Submitted on 25 Feb 2014

HAL is a multi-disciplinary open access archive for the deposit and dissemination of scientific research documents, whether they are published or not. The documents may come from teaching and research institutions in France or abroad, or from public or private research centers.

L'archive ouverte pluridisciplinaire **HAL**, est destinée au dépôt et à la diffusion de documents scientifiques de niveau recherche, publiés ou non, émanant des établissements d'enseignement et de recherche français ou étrangers, des laboratoires publics ou privés.

Vulnerability of a reinforced concrete wall loaded by a snow avalanche: experimental testing and FEM analysis

Ousset I.1*, Bertrand D.2, Brun M.2, Limam A.2 and Naaïm M.1
1 Irstea Grenoble, France
2 INSA Lyon, LGCIE, France

ABSTRACT: In 1999 and 2006, in the Chamonix valley (France,74), a protective device dedicated to deflect and stop snow avalanches was partially destroyed. Experimental pushover tests on a 1/6 scale model have been performed in 2005 to better understand the reasons explaining the failure mode of the defense structure. In this paper, a Finite Element (FE) model is presented and calibrated on the experimental data. Then, the FE model is used to investigate the mechanical response of a reinforced concrete structure under dynamic avalanche loading. Finally, the physical vulnerability of the structure is assessed by a suitable damage index.

KEYWORDS: Snow avalanche defense structure, reinforced concrete, civil engineering, finite element method, vulnerability.

RESUME : Suite aux avalanches qui se sont produites en 1999 puis en 2006 dans la vallée de Chamonix (France, 74), des ouvrages de protection en béton armé ont été endommagés. Afin de mieux comprendre la nature des dégâts observés, des essais de type pushover ont été réalisés en 2005 sur un modèle réduit à l'échelle 1/6 ème. Dans cet article, un modèle numérique aux éléments finis est décrit et le calage effectué sur les données expérimentales. Ce modèle est ensuite utilisé en vue d'investiguer la réponse d'une structure réelle en béton armé sollicitée par un chargement dynamique dû à un écoulement avalancheux. Pour finir, la vulnérabilité physique de la structure est évaluée selon un indice de dommage approprié.

MOTS CLES : Ouvrage paravalanche, béton armé, génie civil, méthode des éléments finis, vulnérabilité.

1 CONTEXT

Snow avalanches threaten more and more structures and housings in mountainous regions, where the lack of space and the urbanization development lead to increase the occupation of exposed area. In the framework of risk analysis, the assessment of risk must take into account on the one hand the hazard and on the other hand the vulnerability assessment of the exposed structures. Nowadays, civil engineering structures exposed to snow avalanches are mostly designed considering static loadings involving large safety factors (Ancey, 1996; Givry and Perfetini, 2006). The latter highlight the lack of knowledge on the effects of the loading

generated by a snow flow, and generally lead to overdesign the civil structures. However the case of the avalanche events in Tacconnaz, in the Chamonix valley, which occurred in 1999 and 2006 and where important parts of defense structures were destroyed, showed that static design approaches seems to underestimate the potential effect of the snow flow (Berthet-Rambaud et al., 2007).

Thus, the objective of this study is to better understand the behaviour of RC (reinforced concrete) structures under snow avalanche loading, considering an L-shaped wall submitted to a dynamic signal coming from in field data measured inside a snow flow (Thibert et al., 2008).

2 STUDIED STRUCTURE

The structure considered in the present study is a concrete L-shaped wall.

* *Corresponding author address:* Ousset I., Irstea, UR ETGR, 2 rue de la Papeterie - BP 76, F-38402 Saint-Martin-d'Hères, France,
Tel: + 1 047 676 2764; Fax: +1 047 651 3803;
Email: isabelle.ousset@irstea.fr

The 1/6 scale structure consists of 1,6 meters concrete height, 1,0 m width, 2,5 m length and 0,25 m thickness (Figure 1 and Table 1). It is reinforced by steel rebars of diameters included between 6 et 12 mm disposed as shown in Figure 1. Steel layers are spaced out of 12 cm in the length direction.

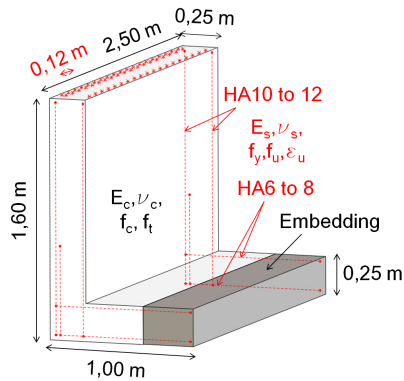


Figure 1: Experimental 1/6 scale model

This structure is inspired of the deflective walls (Figure 2) of the protective device situated in the avalanche path of Taconnaz, which have been partially destroyed in 1999 and 2006. When the avalanche enters inside the area of the defense structure, the shelders allow spreading out the avalanche flow. Then, mounds slow down the flow velocity before the avalanche impacts the dam dedicated to stop its progression.



Figure 2: Taconnaz wall partially destroyed in 1999 (photo courtesy of F. Rapin, Irstea)

3 EXPERIMENTAL RESULTS

Experimental push-over tests on a physical 1/6 scale model (Figure 1) have been performed at the INSA's laboratory in 2005, in order to understand what happened in Taconnaz. Those tests are presented in details by (Berthet-Rambaud et al., 2007). They consisted in applying a uniform distribution of pressure varying linearly over time until the total

collapse of the wall. In the same time, the material's properties (Table 1) have been measured to obtain a complete and accurate experimental database.

The experimental results are presented in Figure 3. The latter describes the horizontal displacement measured on the top of the vertical wall in three different points (middle and extremities) all over the push-over loading.

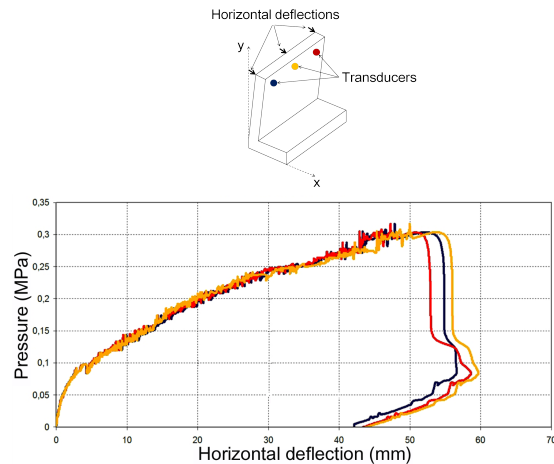


Figure 3: Deflections measured on the top of the vertical wall

4 NUMERICAL MODELLING

4.1 Finite element method

In order to investigate the mechanical response of the structure, a 2D model using the finite element approach has been performed. The Cast3M code has been used (Millard, 1993) to solve the following equation governing the mechanical system: $M \ddot{u}(t) + C \dot{u}(t) + F_{int}(u, \dot{u}) = F_{ext}$ where M is the mass matrix, C the damping matrix, F_{int} the internal forces, F the applied load and u the unknown displacement field. Under quasi-static conditions, the first two terms of the equation equal to zero and for linear systems, $F_{int} = K u$ where K is the stiffness matrix. The meshes of concrete and steel which constitute the structure are presented in Figure 4.

4.2 Boundary conditions and Loading

According to the experimental conditions, the 1/6 scale model is clamped over 35 % of the base length (Figure 4a). A uniform pressure field is ap-

Parameter	Symbol	Value	Unit
Vertical wall geometry			
Height	h	1,60 or 9,60	m
Thickness	e_p	0,25 or 1,50	m
Length	L	2,50 or 14,80	m
Base geometry			
Width	h	1,00 or 6,00	m
Thickness	e_p	0,25 ou 1,50	m
Length	L	2,50 or 14,80	m
Concrete properties			
Young's modulus	E_c	from 38842 to 38925	MPa
Poisson's ratio	ν_c	from 0,18 to 0,3	-
Compressive strength	f_c	from 68,4 to 78,3	MPa
Tensile strength	f_t	from 6,5 to 6,8	MPa
Steel properties			
Young's modulus	E_s	217000	MPa
Poisson's ratio	ν_s	0,3	-
Yield strength	f_y	575	MPa
Ultimate tensile strength	f_u	620	MPa
Ultimate strain	ϵ_u	0,037	-

Table 1: Geometry and mechanical properties of the structure in the 1/6 and full scale

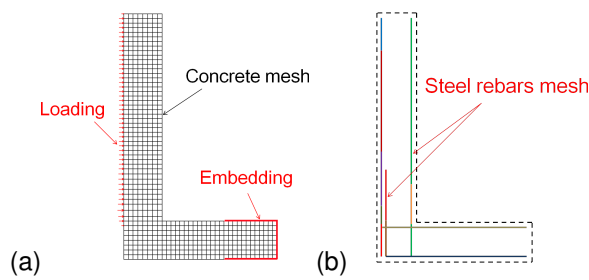


Figure 4: (a) Mesh of concrete and Boundary conditions (b) Mesh of steel rebars

plied onto the totally height of the exposed face to the snow avalanche (Figure 4a).

4.3 Constitutive laws

4.3.1 Concrete

Four constitute laws of concrete (Figure 5) have been tested:

- *Damage elastic model*

The model used here is the Mazars's model (Mazars, 1986). It's an elastic damage model, based on the damage theory, which allows to describe the loss of stiffness due to appear of micro-crakings in concrete. The evolution of the mechanical characteristics is generally anisotropic; so, the damage variable is in that case a tensor. In order to reduce the number of variables, Mazars chose an isotropic damage evolution which leads to a scalar damage variable D , divided into 2 parts: one part

D_t due to tensive strains and an other D_c due to compressive strains. The Young's modulus of concrete is then replaced by $E_c(1 - D)$.

- *Non cyclic elasto-plastic law*

This model is a concrete model in plane stresses proposed by the French CEA's research center. It's an elasto-plastic model first developed by (Nahas, 1986) and then modified by (Leprêtre et al., 1988). The yield limit is described by two yield criteria: Rankine's criterium for the tensive cracking and Drucker-Prager's criterium for compression and bi-compression. The theory of maximal plastic work is used to describe the plastic flow in tension whereas the flow is associated with a rule of isotropic strain hardening for compression.

- *Cyclic elasto-plastic law*

The model used in this case is a law developed at INSA in Lyons by (Merabet, 1990) and extensively used in the last decade for engineering structures submitted to seismic loading (Ile and Reynouard, 2000, 2005). When the state of the concrete is uncracked, the classical plasticity theory is used with an isotropic hardening and an associate flow rule. The crack detection surface follows two Nadai's criteria. The first one is dedicated for tension and the other one for compression and bi-compression. The crack state of the concrete is initiated when the crack detection surface is reached in tension. A virtual crack is created perpendicularly to the principal stress direction and its direction is kept constant until the end of the simulation (smeared and fixed crack theory). A second crack can appear only perpendicularly to the last

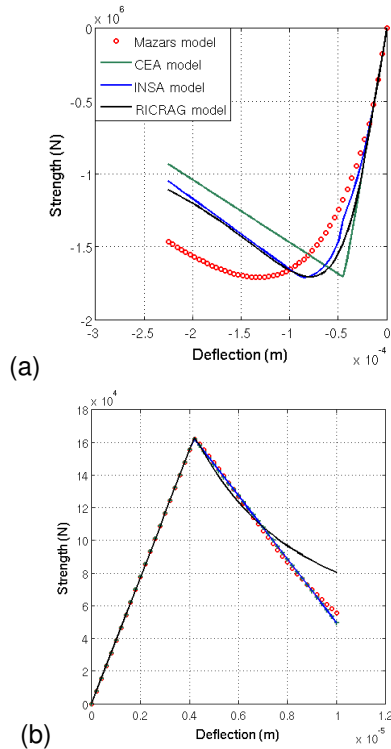


Figure 5: Concrete uniaxial behaviour in (a) compression and (b) tension (on a single finite element)

one. This model allows also to take into account the cyclic effect of a loading using a technique of stiffnesses restoration after cracks closure.

- *Elasto-sliding damage law*

The tested RICRAG model (Richard, 2010) has been developed in order to describe the behaviour of concrete under seismic loadings. It's a model coupling elasticity, isotropic damage and internal sliding. It takes into account openings and closures of cracks as well as sliding and friction mobilized between the lips of cracks. It is thus adapted to the cases of alternated monotonous and cyclic loadings.

4.3.2 Steel

An elasto-plastic law with a little strain hardening, calibrated on the experimental data presented in Table 1, describes the steel behaviour (Figure 6) and a perfect joining between concrete and steel has been supposed.

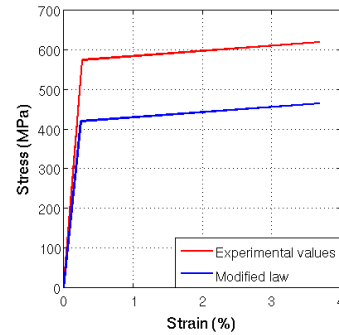


Figure 6: Steel behaviour law

5 VULNERABILITY CURVES

In the framework of risk analysis, a vulnerability curve is a monotonous curve with values ranging between 0 and 1 describing the variation of a damage index according to the natural hazard intensity. The damage index I makes it possible to quantify the structure vulnerability for a given hazard. When the structure is not damaged, $I = 0$. The strains inside the structure remain in the elastic domain. On the other hand, $I = 1$ corresponds to the total destruction of the structure.

In the case of avalanche loading, vulnerability curves can be derived varying the maximal pressure applied on the structure (P_{max}). Experimental measurements from several authors (Berthet-Rambaud et al., 2008; Sovilla et al., 2008, 2010; Thibert et al., 2008; Thibert and Baroudi, 2010; Baroudi et al., 2011) permit to give the order of magnitude of the pressure developed by a snow avalanche on a structure. Usually, the pressure of a dense snow avalanche vary between 20 and 600 kPa (Tacnet et al., 2010).

6 RESULTS

6.1 Numerical calibration

The numerical model has been first calibrated with the CEA's constitutive law in order to obtain the same results as those of the experimental test presented in Figure 3. The dimensions of the numerical model are in that case those of the 1/6 scale model presented in Figure 1 and in Table 1. The applied load varies linearly from 0 to 35 kPa with a loading step of 350 Pa, until the collapse of the structure. The calculation is conducted under quasi-static conditions (same as the experimental test): so, $F_{int}(t) = F_{ext}(t)$.

A parametric study on material characteristics allows highlighting the influence of the different parameters on the mechanical response of the structure (Figure 7).

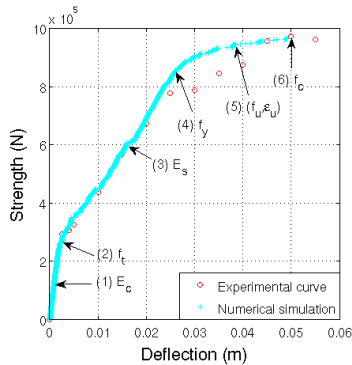


Figure 7: Influencing parameters on the different damage levels for the CEA's model

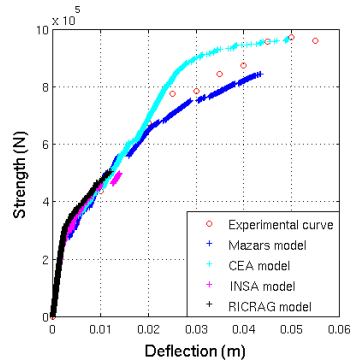


Figure 8: Calibration results of the different models (pushover loading)

In order to obtain a good calibration, the tensile strength of concrete has been taken equals to 6 MPa and steel characteristics have been decreased as shown in Figure 6 ($E_c = 170000$ MPa, $f_y = 400$ MPa and $f_u = 445$ MPa).

Uniaxial tension and compression tests on a single finite element have been then simulated in order to calibrate the different constitutive laws (Figure 5).

The calibration results on the experimental pushover test are plotted in Figure 8. Only the two models of Mazars and CEA allow obtaining the total collapse of the structure. The convergence is not obtained for the other two models.

Non linear constitutive laws moreover allows obtaining the collapse mode as shown as Figure 9. While the CEA's model provides values of pressure and deflection closer to the reality than the Mazars's model, the latter provides on the other hand a better description of the collapse mode.

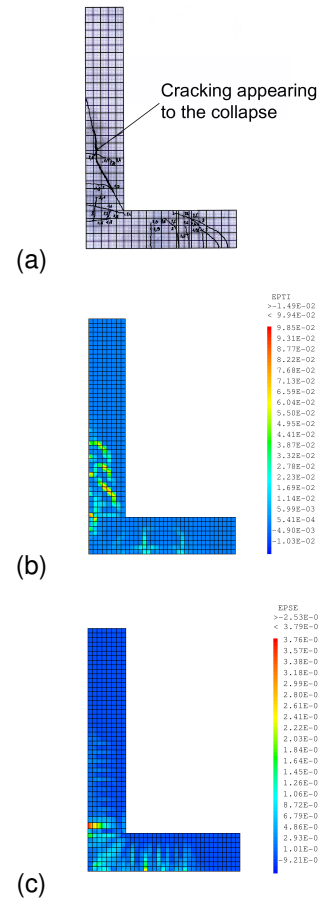


Figure 9: Cracking observed (a) experimentally, (b) with the Mazars's model and (c) with the CEA's model

As far as the most important parameters for the following are values of pressure and deflection, the retained model is the CEA's model. Furthermore, the Mazars's model is more sensitive to the step of calculation and to the mesh.

6.2 Full scale structure modelling under avalanche loading

The calibration of the FE model allows exploring the behaviour of the in-situ RC wall located in Taconnaz. Thus, the structure studied in this paragraph corresponds to the real structure, whose base is longer (Table 1) and totally clamped.

First, a pushover test has been performed, in order to obtain the capacity of the structure in terms of strength-displacement response.

In a second time, a modal analysis has been conducted: the first natural frequency obtained by the

numerical model is: $f_1 = 14,5$ Hz. The latter value of frequency seems to be very high compare to usual values found for classical civil RC structures. However, the considered structure is highly reinforced and its dimensions are rather small. Thus, the characteristic time of the structure response is about $t_{car} = t_1 = 1/f_1 = 0.069$ s.

Finally, an in-situ measured snow-dense avalanche loading (Thibert et al., 2008) is applied on the RC wall. The aim is to explore the response of the structure under this particular dynamic loading. The measurements come from an experimental test site of IRSTEA located in France and are presented in Figure 10a. The pressure is supposed constant along the vertical direction and the time evolution is plotted in the Figure 10b.

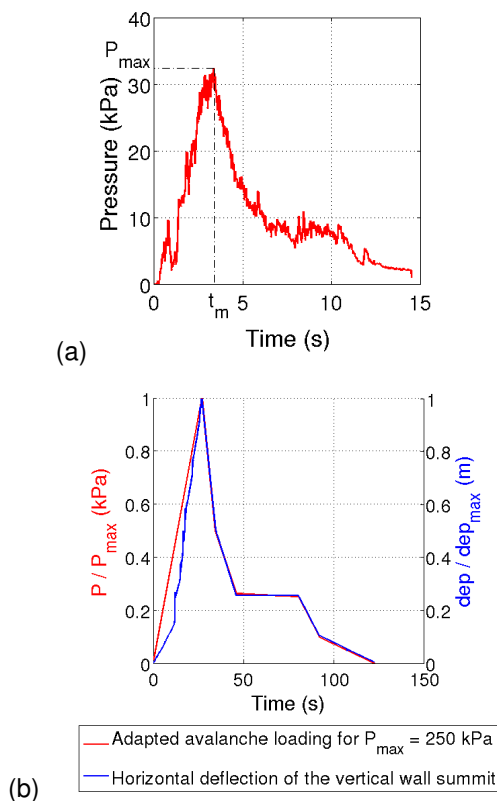


Figure 10: (a) The pressure signal used in the FE simulation is deduced from in-situ measurements. (b) The structural response is described in terms of displacement as a function of time. In the simulation, $P_{max} = 250$ kPa.

Simulations have been carried out under dynamic conditions. Figures 10b show that the response of the structure seems to be quasi-static when this kind of loading signal is applied. Indeed,

the loading rate is much higher than t_{car} which explains that the response is quasi-static.

6.3 Parametric study

Finally, the influences of the loading and the structure features on the mechanical response have been explored. First, the loading rate and the maximal pressure reached are considered. Then, the influence of the reinforcement density is presented.

6.3.1 Loading

- Rise time (t_m)

The rise time (t_m) is defined as the time needed to reach the maximal pressure during the loading. In figure 11, several values of t_m are used and compared to t_{car} . As long as $t_m \gg t_{car}$, the force-displacement curve fits the curve obtained from the pushover test. Thus, the structure response is quasi-static. Dynamic effects appear for much smaller rise times.

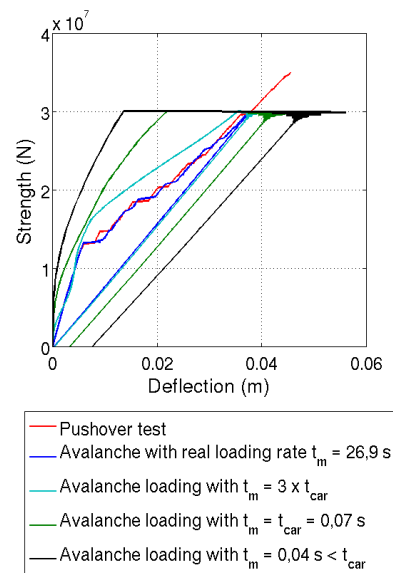


Figure 11: Structure response to several snow avalanche loadings where the rise time (t_m) is changed. t_{car} represents the characteristic time of the structure.

One note that these results are only valid in this particular study involving in field measurements coming from dense avalanche flows (Thibert et al., 2008).

- Pic pressure (P_{max})

For this parametric study, the maximum pressure has been varied keeping constant the loading rate, i.e. P_{max}/t_m .

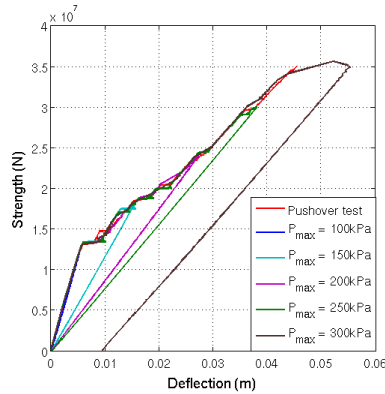


Figure 12: Influence of P_{max} on the structure response

In figure 12, the response of the structure is elastic for pic pressures lower than 100 kPa. For higher pressures, material non linearities develop. Because the loading rate is constant and estimated from in field data (i.e. low loading rate), the mechanical response is still quasi-static.

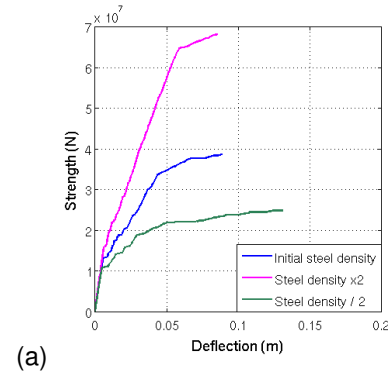
6.3.2 Structure

Concerning the structure, the influence of the reinforcement density has been investigated. In addition, the assessment of the physical vulnerability of the RC wall has been proposed.

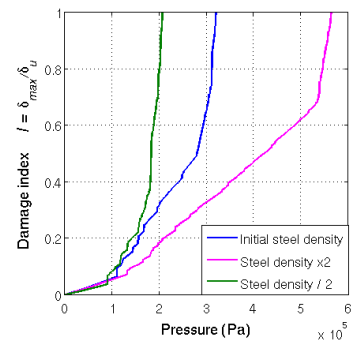
In figure 13a, three pushover tests are presented for several steel densities. The RC wall response depends significantly on this parameter. For RC civil engineering structure, the failure mode is mainly controlled either by the crushing of the concrete under compression or the rupture of the steel. For high (resp. low) steel densities, the structure collapse is due to the concrete crushing (resp. rebar's rupture).

In order to quantify the vulnerability of the structure, a global damage index (I) is here defined. $I = \delta_{max} / \delta_u$ where δ_u is the ultimate displacement of the structure before collapse and δ_{max} the maximum displacement of the structure during a given loading. The pushover tests represent the capacity of the structure and allow determining δ_u . Figure 13b depicts the vulnerability curves. Vulnerability is higher for low steel densities. Indeed, on the one

hand the ultimate pressure is lower, but on the other hand steel yielding leads to a steeper vulnerability curve. Beyond 180 kPa, a light increase of pressure implies a huge increase of I .



(a)



(b)

Figure 13: (a) Influence of steel density on the structure capacity (b) Vulnerability curves

7 CONCLUSION and PERSPECTIVES

In order to better understand the behaviour of RC structures submitted to dense snow avalanches and to study their vulnerability to such hazards, experimental quasi-static tests on a 1/6 scale physical model have been carried out. A finite element model is proposed and calibrated from these experimental tests. The influence of the avalanche loading has been investigated under dynamic conditions. The response of the studied structure to a loading coming from a dense avalanche seems to be quasi-static. We also have performed a parametric analysis on the material characteristics and proposed vulnerability curves. The influence of the reinforcement density has been explored. The failure mode is very sensitive to that parameter and thus has a significant influence on the vulnerability

of the structure. For low steel densities, the collapse can arise very quickly after the beginning of the steel yielding. It is not the case when concrete crushing is responsible for the failure. Indeed, in that case, the gradient of the vulnerability curve is lower.

Concerning the perspectives, the effects of the geometry will be studied from a deterministic point of view (boundary conditions, wall thickness, rebars position, etc.). The aim will be to identify the most influent parameters in the structure response.

Next, accounting for the uncertainties related to natural hazards and civil engineering constructions, fragility curves will be derived in a reliability framework (FROM, Monte Carlo simulation, etc.) and the failure probability of the structure will be assessed.

Finally, the approach will be extended to structures such as multi-storey buildings. Indeed, these kind of structures are higher and less stiff than protective structures. Thus, the natural frequencies are lower and dynamic effects can appear and should be taken into account.

8 REFERENCES

- Ancey, C., 1996. Guide neige et avalanches : connaissances, pratiques, sécurité. Edisud.
- Baroudi, D., Sovilla, B., Thibert, E., 2011. Effects of flow regime and sensor geometry on snow avalanche impact-pressure measurements. *Journal of Glaciology* 57, 277–288.
- Berthet-Rambaud, P., Limam, A., Baroudi, D., Thibert, E., Taillandier, J.M., 2008. Characterization of avalanche loading on impacted structures : a new approach based on inverse analysis. *Journal of Glaciology* 54, 324–332.
- Berthet-Rambaud, P., Limam, A., Roenelle, P., Rapin, F., Tacnet, J.M., 2007. Avalanche action on rigid structures : Back-analysis of taconnaz deflative wall's collapse in february 1999. *Cold Regions Science and Technology* 47, 16–31.
- Bertrand, D., Naaïm, M., Brun, M., 2010. Physical vulnerability of reinforced concrete buildings impacted by snow avalanches. *Natural Hazards and Earth System Sciences* 10, 1531–1545.
- Givry, M., Perfetini, P., 2006. Construire en montagne : la prise en compte du risque d'avalanche. Ministère de l'Ecologie et du Développement Durable.
- Ile, N., Reynouard, J.M., 2000. Nonlinear analysis of reinforced concrete shear wall under earthquake loading. *Journal of Earthquake Engineering* 4, 183–213.
- Ile, N., Reynouard, J.M., 2005. Behaviour of u-shaped walls subjected to uniaxial and biaxial cyclic lateral loading. *Journal of Earthquake Engineering* 9, 67–94.
- Leprêtre, C., Millard, A., Combescure, A., Jamet, P., 1988. Calcul à la ruine des structures en béton armé - Mise au point d'un modèle béton en contraintes planes. Report DEMA 88/330. Atomic Energy Commission, Saclay, France.
- Mazars, J., 1986. A description of micro- and macroscale damage of concrete structures. *Engineering Fracture Mechanics* 25, 729–737.
- Merabet, O., 1990. Modélisation des structures planes en béton armé sous chargements monotone et cyclique. Ph.D. thesis. National Institute for Applied Sciences, Lyon, France.
- Millard, A., 1993. CASTEM 2000, Manuel d'utilisation. Report CEA-LAMBS 93/007. Atomic Energy Commission, Saclay, France. www-cast3m.cea.fr.
- Nahas, G., 1986. Calcul à la ruine des structures en béton armé. Ph.D. thesis. Applied Sciences University Paris VI.
- Richard, B., 2010. Isotropic continuum damage mechanics for concrete under cyclic loading : Stiffness recovery, inelastic strains and frictional sliding. *Engineering Fracture Mechanics* 77, 1203–1223.
- Sovilla, B., Kern, M., Schaer, M., 2010. Slow drag in wet-snow avalanche flow. *Journal of Glaciology* 56, 198.
- Sovilla, B., Schaer, M., Kern, M., Bartelt, P., 2008. Impact pressures and flow regimes in dense snow avalanches observed at the vallée de la sionne test site. *Journal of Geophysical Research* 113, F01010.
- Tacnet, J.M., Thibert, E., Berthet-Rambaud, P., Limam, A., Naaïm, M., Perrotin, P., Richard, D., 2010. Conception et comportement dynamiques des structures de génie civil : application aux ouvrages paravalanches. *Sciences Eaux et Territoires* 2, 46–57.
- Thibert, E., Baroudi, D., 2010. Impact energy of an avalanche on a structure. *Annals of Glaciology* 51.
- Thibert, E., Baroudi, D., Limam, A., Berthet-Rambaud, P., 2008. Avalanche impact pressure on an instrumented structure. *Cold Regions Science and Technology* 54, 206–215.